

MONTE CARLO SIMULATIONS OF THE THERMAL DENATURATION TRANSITION OF MODEL DNA CHAINS IN SOLUTION

Juan C. Araque¹, **Athanassios Z. Panagiotopoulos**⁴ and **Marc A. Robert**^{1,2,3}

¹Department of Chemical and Biomolecular Engineering, ²Rice Quantum Institute, ³Richard E. Smalley Institute for Nanoscale Science and Technology, Rice University, Houston, TX, USA

⁴Department of Chemical Engineering, Princeton University, Princeton, NJ, USA

Abstract

The thermal denaturation (melting) of DNA molecules is a thermodynamic and conformational order-disorder transition from a double-stranded to a single-stranded state. Modeling DNA melting at the atomistic level is severely hampered due to the time and length scales of this transition. We propose a coarse-grained model where DNA strands are represented as oligomer chains of N beads using the single-site bond-fluctuation model on a cubic lattice. This approach incorporates physically relevant characteristics such as the sequence and orientation dependence of base-stacking and base-pairing interactions, as well as the semiflexibility of the chains. We perform parallel tempering Monte Carlo simulations of dilute solutions of short DNA strands in the canonical ensemble. Due to the strong short-ranged and anisotropic nature of the interactions, we employ various biased trials to improve the phase-space sampling. Feedback optimization of the temperature distribution and multihistogram reweighting techniques were used to obtain accurate estimates of the transition temperature. This procedure allows the direct calculation of thermodynamic and conformational properties across the thermally induced order-disorder transition. We explore how the interaction heterogeneity, broad stacking transition and chain stiffness may induce specific heat capacity effects, shift the location of the melting temperature and broaden the transition. Overall, the phenomenological behavior predicted is in qualitative agreement with experimental observations.

Introduction

The opening and winding of double stranded DNA is a ubiquitous phenomenon in biological systems. Processes involving replication and transcription of DNA require a localized unwinding and renaturation for every region of its sequence. The accurate prediction of the DNA melting temperature (T_m) is of tremendous importance in the experimental performance and outcome of several molecular biology techniques including genome sequencing, expression (microarrays) and amplification (PCR) methods [1]. In recent years, DNA recognition properties are becoming increasingly important for biosensors applications and biologically conjugated nanomaterials for nanotechnology applications [2].

Understanding the principles governing double helix formation is essential for understanding and predicting the properties of nucleic acids in general [3]. Thermodynamic studies on short sequences of DNA (also known as oligonucleotides) provide a convenient way for discovering these principles and facilitate the rational design of sequences for the various applications mentioned above [4]. Melting experiments of oligonucleotides have attracted a vast amount of experimental and theoretical research since the late 1950's and early 1960's [5]. In addition to experiments and theory, a comprehensive understanding of

the thermodynamic behavior of this process can be achieved by computer simulation methods. However, as commonly occurs with complex associating or self-assembling systems [6], e.g., spontaneous micelle formation in surfactant solutions, the time and length scales of the collective behavior of DNA melting in solution (even for the case of oligomers) are not accessible to atomistic simulations. A novel molecular simulation approach proposed here aims to deal with fundamental aspects related to the thermally-induced denaturation transition of oligomer DNA strands in solution. This approach couples a simple and computational efficient lattice model in three dimensions with advanced computer simulation techniques based on the Monte Carlo method.

In this article, we present a multicanonical Monte Carlo simulation study of model DNA chains. We first describe the details of the lattice model implemented. We next explain briefly the methodologies employed to study the thermodynamical stability of the model chains across the denaturation transition. In the following section, we present and discuss the results obtained for different case studies. In the last section, we summarize the main conclusions from this study.

Model

We consider a solution with M oligomer chains of N beads (where $N < 16$). The system is composed of an equimolar binary mixture of single strands with full or partial complementarity. The space is discretized into a three-dimensional simple cubic lattice with volume $V = L^3$, where L is the length of the simulation box. Periodic boundary conditions are implemented in all three dimensions. Single-stranded DNA chains are modeled by a sequence of connected lattice sites, where each nucleotide (base and sugar-phosphate backbone) represents a single monomer unit. The monomer beads, with diameter σ equal to the lattice spacing, are connected following the single-site bond fluctuation model with a coordination number of $z = 26$. Therefore, successive beads on a chain are joined by a vector from the set $(0,0,1)$, $(0,1,1)$ and $(1,1,1)$ and equivalent vectors resulting from reflection operations on the cubic lattice. This coordination number is higher than that of the simple cubic lattice ($z = 6$), which means that the chain not only has greater bending angles available but also three possible bond lengths with values of 1, $\sqrt{2}$ and $\sqrt{3}$ lattice units. Monomeric solvent particles are assumed to fill all the lattice sites not occupied by chain segments; however, the solvent is not explicitly taken into account, i.e., solvent-solvent and solvent-nucleotide energy parameters (ϵ_{ss} and ϵ_{sn}) are set to zero. This implies that the strands are assumed to be in a θ -solvent, which is a reasonable assumption for DNA in most aqueous solutions [7].

The thermodynamic stability of DNA oligomers depends strongly on base composition and sequence. In our implementation, the heterogeneity in the monomer distribution along the chains is explicitly incorporated by considering four different nucleotides units representing the purine and pyrimidine bases: adenine (A), thymine (T), cytosine (C) and guanine (G). Hence, our model strands could be thought as heteropolymer lattice chains with a sequence space comprised of four letters (A, T, C and G), arranged in a prespecified order which is not necessarily random in nature since DNA carries genetic information. The DNA lattice chains are labeled with a predefined direction between the 3' and 5' ends, such that the double-stranded sequence complementarity runs in opposite directions. Hence, antiparallel association is only the result of the imposed order

in the sequence, and does not originate from any sterical constraints as for real nucleic acids. It should be noted that in this discretized model, although highly computationally efficient, the detailed chemical structure of the double-helix conformation is completely neglected. Nevertheless, lattice models have been extensively applied because they are known to retain universal features of polymers [7].

All lattice chains considered in this model are mutually- and self-avoiding, so that hard-core monomer beads interact directly by exclude volume. The anisotropic hydrogen bonding interactions, resulting from neighbor pairs of complementary monomers, are included explicitly as associating sites pointing in any of the $z = 26$ directions. Thus, a pair of free lattice beads is allowed to bind only when they are in neighboring positions (square-well type potential) and their hydrogen-bonding sites are oriented towards each other. Each monomer can interact only with one monomer at a time, so the bond is said to be saturating. The base-pairing energy parameters $\epsilon_{HB,ij}$, where the pair ij can be any combination of the four nucleotides, is represented by a WC-pairing compliant matrix. Intra-chain base-stacking is also considered explicitly by a favorable interaction for consecutive beads with bonding sites pointing in the same direction. The matrix elements of the stacking energy parameter $\epsilon_{ST,ij}$ take into account the heterogeneity of the sequence. All energy parameters (scaled with respect to $\epsilon_{HB,AT}$) come from the most accurate quantum mechanical calculations in the gas phase to this date [8,9]. However, we have introduced an additional *ad-hoc* rescaling of the stacking energies to account for the solvation effects and higher stability with respect to the hydrogen-bonding in aqueous solution. The reduced temperature is then defined as $T^* = k_B T / \epsilon_{HB,AT}$, where T is the absolute temperature and k_B Boltzmann's constant. To model the conformational change in chain stiffness associated with the melting transition, we include a bending potential between successive bond vectors as in previous models for stiff lattice homopolymers and surfactant chains [11, 12]. The bending parameter in this potential was adjusted with trial runs in order to reproduce approximately the persistence length of the single- and double-stranded DNA at low and high fraction of association, respectively.

In order to simplify the configurational sampling of phase space, we assume neutral chains. Therefore, electrostatic interactions are not included either explicitly or implicitly. Although clearly an oversimplification, since DNA strands are negatively charged polyelectrolytes, theoretical studies have already considered that the total melting free energy may well be expressed as uncoupled contributions from electrostatic and non-electrostatic interactions, which are computed separately [13]. Moreover, coarse-grained continuous molecular dynamics (MD) simulation models have neglected the electrostatic contributions in order to decrease the number of degrees of freedom and have access to the time-scale of hybridization events for a single pair of strands [14,15]. Nevertheless, we opted to simulate dilute solutions in all cases, i.e., well below the overlap threshold φ^* defined as $\varphi^* = N/(4/3\pi R_g^3)$, where R_g is the radius of gyration. At these conditions, minimal electrostatic interactions between DNA strands are expected in well-screened solutions.

Simulation Methods

The Monte Carlo (MC) simulations were performed in the canonical ensemble where the temperature, number of chains and volume are held constant (*NVT*) [16]. The

length of the simulation box used (L) is selected such that it is at least 10 times larger than the radius of gyration of the strands at the largest extension. We implemented a mixture of biased trials that bridge the slow and fast relaxation events. For the short time-scales, we apply orientational/rotational bias (OB) [17] on all hydrogen-bonding sites on a randomly selected chain. A combined orientational and configurational bias (CB) [18] half-chain regrowth represents the medium time-scales moves. For long-time scales, we implement an orientational and configurational bias full-chain regrowth at a randomly selected position for the first bead. For all cases, the configurational bias sampling for chain regrowth is based purely on the bending potential. Additionally, the orientational bias moves consider stacking and pairing interactions. This particular decoupling choice allows us to achieve a significant reduction of the slowdown associated to the joined thermal implementation. Thus, the biased acceptance criteria include a composite Rosenbluth weight, which takes into account the chain stiffness during growth and all orientation-dependent interactions.

For any given system, several different temperatures across the transition must be simulated until the complete melting curve is obtained. However, at low temperatures and dilute conditions, the anisotropic and short-ranged associating nature of the model interactions imposes severe restrictions on the phase-space sampling. This is a typical problem for molecules associating via hydrogen-bonding. There is an intrinsic competition between the low probability of placing the strands in favorable pairing configuration and then escaping from bound states once formed [19]. In order to overcome the high free energy barriers linked to low-temperature systems, we resort to the generalized or multicanonical ensemble technique called parallel tempering or replica exchange [20]. Therefore, in addition to the regular Metropolis [21], we also perform a random walk in temperature space. In this scheme, a defined number of NVT replicas at different temperatures (with $T_1 < T_2 < \dots < T_P$) are simulated in parallel. Configurational swaps or exchanges between neighboring replicas are proposed after a specified number of MC cycles [22]. Replica exchanges are accepted or rejected following the appropriate acceptance criteria. We use a fixed number of 16 replicas for all systems studied and the initial temperature distribution is set according to a geometric progression (as commonly used in the literature [19]).

The thermal denaturation of DNA molecules exhibits a pronounced peak in the specific heat right at the transition temperature (similarly to helix-coil transitions for polypeptides). This phenomenon has a profound effect on the acceptance probability of parallel tempering moves, as has been described elsewhere [23]. The net effect is a bottleneck in the replica diffusivity across the temperature distribution; thus, significantly downgrading the relaxation benefits from swapping high- and low-temperature replicas. Hence, we apply a recently developed method aiming to overcome such problems [24, 25]. This algorithm systematically optimizes the temperature distribution by maximizing the round-trip rates of replicas between the extremal temperatures. For most cases analyzed, three or four iteration steps are necessary to achieve temperature-convergence and considerable improvement in the equilibration of the system. We use this method in combination with multi-histogram reweighting techniques [26, 27] to improve substantially the estimation of the peak of the specific heat and consequently the transition or melting temperature T_m . It should be noted that despite all the combined set of optimized Monte Carlo biased-trials and fast relaxation methods implemented, we are currently limited to simulate relatively short chains (oligomers up to 16 nucleotides). We find prohibiting longer

equilibration CPU times for longer chains as the result of a noticeably drop of the acceptance probabilities (especially for both half- and full-chain regrowth moves)

Results

As a first case study, we simulated an idealized perfect-match hybridization model for DNA strands in solution. This model is intrinsically different to the one described above, but the Monte Carlo algorithm developed is flexible enough as to allow us consider this type of variation. Under this simplification, the chains are considered fully flexible, with no stacking interactions, and the monomer units no longer represent individual nucleotides but statistical segments, which bind to their complementary image on a neighboring strand. However, the model still preserves the directional nature of segment pairing. Each statistical monomer unit can be thought as a Kuhn segment. Therefore, according to the persistence length of single-stranded DNA, it may be comprised of approximately 6 to 20 nucleotides [28] (depending on the sequence, degree of stacking and ionic strength). The perfect-match simplification has been a model subject of mean-field theories and simulation studies since the late 1950's (see [29] and references therein). The underlying approximation has allowed to study the nature of the transition at the thermodynamic limit (or for very large values of N) for a single pair of DNA strands at infinite dilution. Nevertheless, very little attention has been paid to the case of solutions with finite concentration away from the thermodynamic limit of infinite chains.

We simulated a dilute solution of DNA oligomer lattice chains, with lengths $N = 4, 6, 8, 10$ and 12 , on a cubic lattice with box of length $L = 30$ at constant monomer volume fraction $\varphi = 0.0059$. As expected, the chain length has a dramatic influence on the nature of the equilibria. In Fig. 1 we show the behavior obtained for the melting transition with respect to the natural order parameter for this phenomenon, i.e., the total fraction bonded bases $\langle f_{HB} \rangle$. It is clear that it follows the sigmoidal-like continuous transition typically observed for cooperative systems. This is somewhat expected since DNA denaturation (forward) and hybridization (reverse) processes are known to be a classical example of positive cooperativity (as well as many other classical cooperative processes like protein folding, ligand binding and polypeptide helix-coil transitions). As shown in Fig. 2, the melting temperature, defined as the temperature where the specific heat peaks $(C_V/k_B)^{max}$, increases with chain length, whereas the width of the transition becomes narrower for larger values of N . However, instead of observing a significant shift in the location of the melting curves, they exhibit a crossover behavior. Recent results of van Erp *et. al.* [30] using the Peyrard-Bishop-Dauxois (PBD) model, shows indeed the existence of this crossover-type behavior as the melting transition continuously approximates a sharp step function for large N . The characteristic increase and sharpening of the specific heat peak with increasing chain length suggests the possibility of a continuous phase transition (analogous to the behavior of the helix-coil transition for polypeptides [31]). As shown in the inset of Fig. 2, the maximum exhibits a scaling behavior with a nontrivial exponent (calculated from the fit), which gives further evidence for the continuous nature of the transition. We should also note in Fig. 1 that even when there is no favorable energy for stacking the bases on top of each other, the fraction base-stacking $\langle f_{ST} \rangle$ also experiences a transition with no sign of cooperativity. Simulation results shown for this case involved on

average 3 to 4 rounds of feedback optimization of the temperature distributions for all chain lengths.

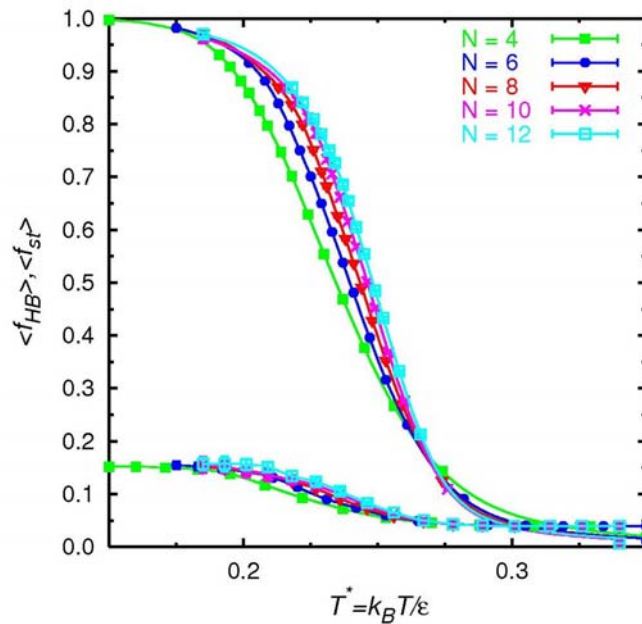


Figure 1. Average fraction of bases bonded $\langle f_{HB} \rangle$ and average fraction of bases stacked $\langle f_{ST} \rangle$ as function of the reduced temperature $k_B T / \epsilon$ for different lattice chain lengths N . The lines represent interpolation from histogram reweighting. Statistical errors are smaller than the size of the symbols.

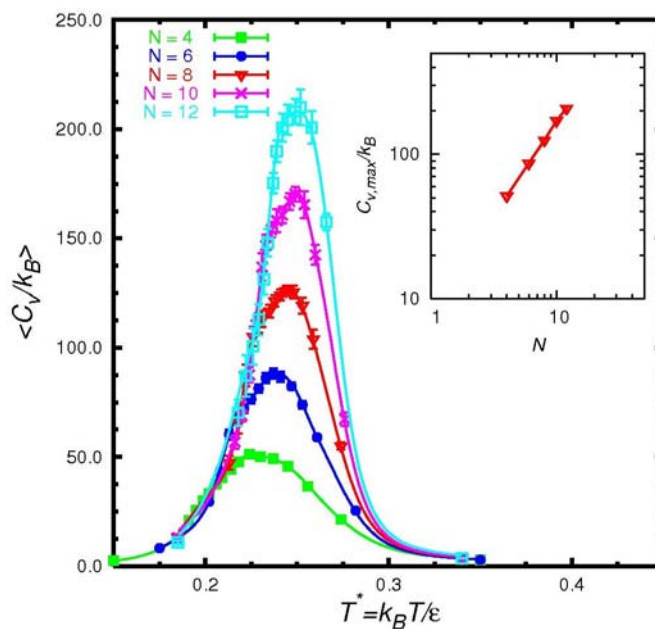


Figure 2. Average specific heat $\langle C_V / k_B \rangle$ as function of the reduced temperature $k_B T / \epsilon$ for different lattice chain lengths N . The lines represent interpolation from histogram reweighting. Statistical errors are typically smaller than the size of the symbols. The inset shows the scaling behavior of the specific heat peak $(C_V / k_B)^{max}$ with respect to the chain length N .

For the model at the nucleotide resolution level, we have performed a similar type of analysis in the multicanonical ensemble including the full set of base-pairing and base-stacking matrices of interactions. The bending potential is also considered as described above to restrict the degree of stiffness of single-stranded DNA chains. We first demonstrate its application on a sample system of oligomer strands with $N=8$ nucleotides units having the self-complementary sequence $(ATCGCGAT)_2$. Simulations were performed on a cubic lattice with box length $L = 30$ at constant monomer volume fraction $\varphi = 0.0059$ ($M = 20$ chains). In Fig. 3 we show the melting and specific heat curves for this system. As in the previous case, the progression of the fraction of bases bonded exhibits positive cooperativity whereas the stacking transition is noticeably broader and shows little if any cooperativity, in agreement with experimental observation [3]. In Fig. 4 we present four snapshots of equilibrium configurations (before and after the transition) at the corresponding temperatures indicated on the melting curve in Fig. 3a. This sequence of images provides a clear picture of the conformational transition coupled to the denaturation/hybridization thermodynamic transition.

From the temperature corresponding to the $(C_v/k_B)^{max}$ in Fig. 3b, an accurate estimate of the melting temperature was obtained for this sequence at the indicated conditions. At this temperature, the corresponding fraction of bases paired is $\langle f_{HB} \rangle_m = 0.364$. This value is significantly smaller than the commonly assumed value in the analysis of UV absorbance plots $\theta = 0.5$ (inflection point of absorbance curve). However, this is not surprising, since the latter has no real thermodynamic meaning but is rather a convenient simplification for the van't Hoff analysis of the experimental data. A test calculation on this same sequence using the DINAMelt server from Zuker et. al. [32] ($[DNA] = 2 \cdot 10^{-5}$ M and $[Na+] = 1$ M) shows that in fact $\langle f_{HB} \rangle \approx 0.30$ at the T_m corresponding to the peak of the heat capacity plot.

In this particular case, we have performed four rounds of feedback optimized parallel tempering to attain an appropriate temperature distribution. The iterative application of this algorithm to the data collected during the simulation allowed us to reduce considerably the error bars of the average specific heat (50 to 100% reduction approximately), especially close to the transition point where the method concentrates a larger number of temperatures. This is a clear indication of the bottleneck effect on the exchange of replicas related to the specific heat peak. A further analysis of the data shows the improvement in the acceptance probabilities of parallel tempering moves as well as the replica diffusivity between the first and last iterations (data not shown). This further confirms the achieved enhancement in the sampling of phase-space. We are also able to observe the direct impact on the refinement of the T_m estimation from the multi-histogram reweighting of the simulation data.

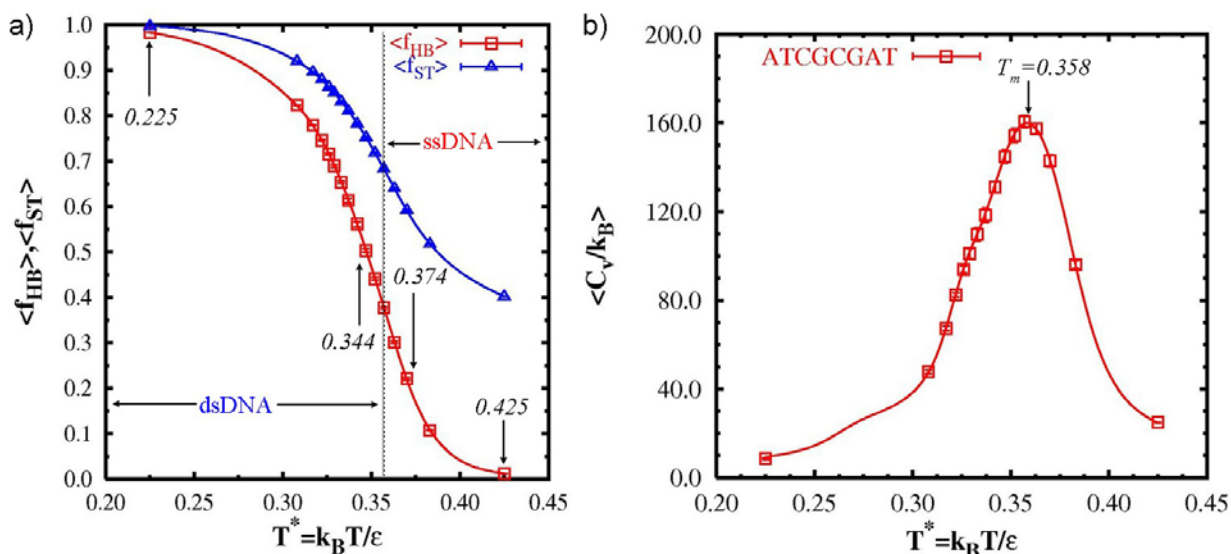


Figure 3. a) Average fraction of bases bonded $\langle f_{HB} \rangle$ and average fraction of bases stacked $\langle f_{ST} \rangle$ as function of the reduced temperature $k_B T / \epsilon$ for the thermal denaturation of the self-complementary sequence $(ATCGCGAT)_2$. b) Average specific heat $\langle C_V / k_B \rangle$ as function of the reduced temperature $k_B T / \epsilon$. Both plots show the precise location of the melting temperature $T_m = 0.358$ in reduced units. The lines represent interpolation from histogram reweighting. Statistical errors are smaller than the size of the symbols.

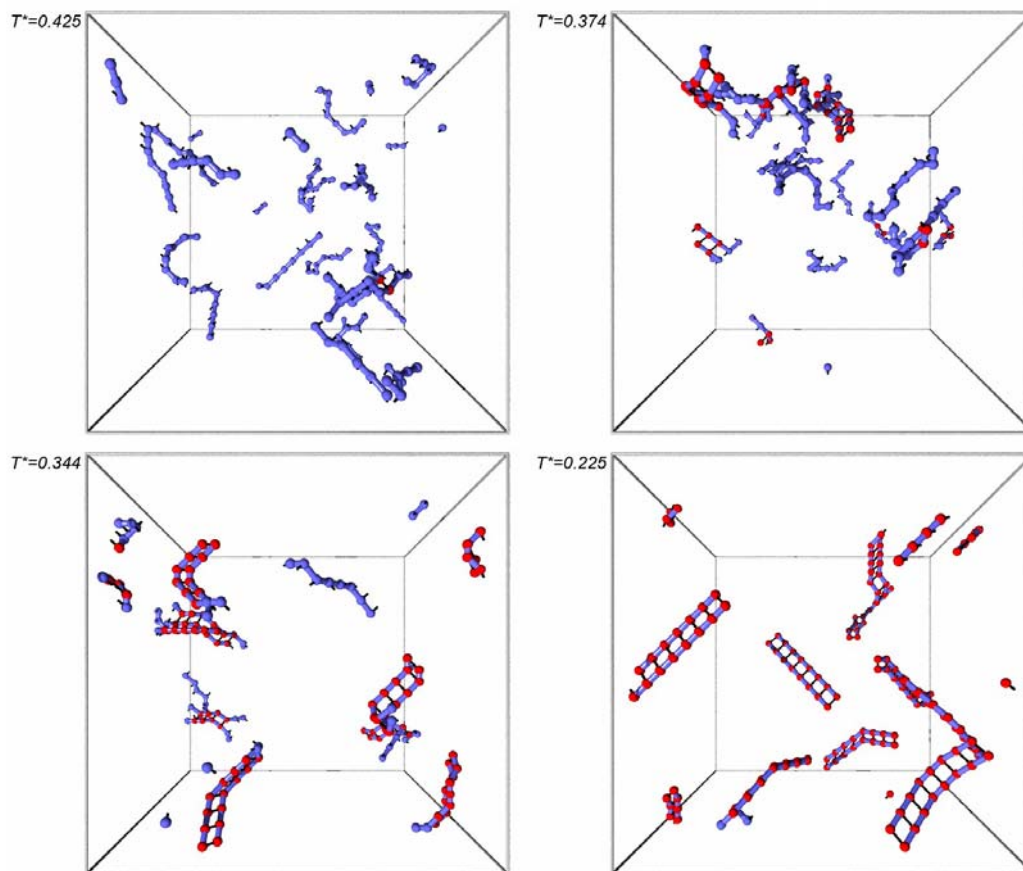


Figure 4. Sample snapshots of equilibrium configurations distributed across the temperature range of the melting transition (as indicated in Fig. 3a). All snapshots correspond to the self-complementary sequence $(ATCGCGAT)_2$. The monomer units colored red correspond to the hybridized bases, whereas the ones colored blue are the unpaired bases. The black pins indicate the direction of the binding and stacking sites.

We evaluated the degree of specificity in the interactions of our model DNA chains in solution by studying the effect of base-pair mismatches on the thermal stability. We introduce errors in the self-complementary sequence already described above, $(\text{ATCGCGAT})_2$, such that we explicitly localize the mismatches at the end, center and middle base-pairs. From the shifts in the melting curves (or specific heat peak), a significant loss of thermal stability is clearly observed for those two cases where the mismatch is located in the center bases or flanking the center base pairs. However, the case of end-mismatch has a negligible effect on the stability. This result corresponds directly to the fact that DNA oligomers denature by unzipping from the ends. This phenomenon is well known from oligomer helix-coil experiments [33], and has been perfectly reproduced by theoretical models based on statistical thermodynamic principles [34, 35, 36]. The effect of unzipping at the ends has also an important kinetic rate contribution, since the dissociation of end base pairs responds to very fast relaxation times (of the order of ns to μs). In addition, the mechanism of association or hybridization from the center base pairs toward the ends has an enhanced equilibrium constant of propagation due to the chain symmetry and stiffness factors.

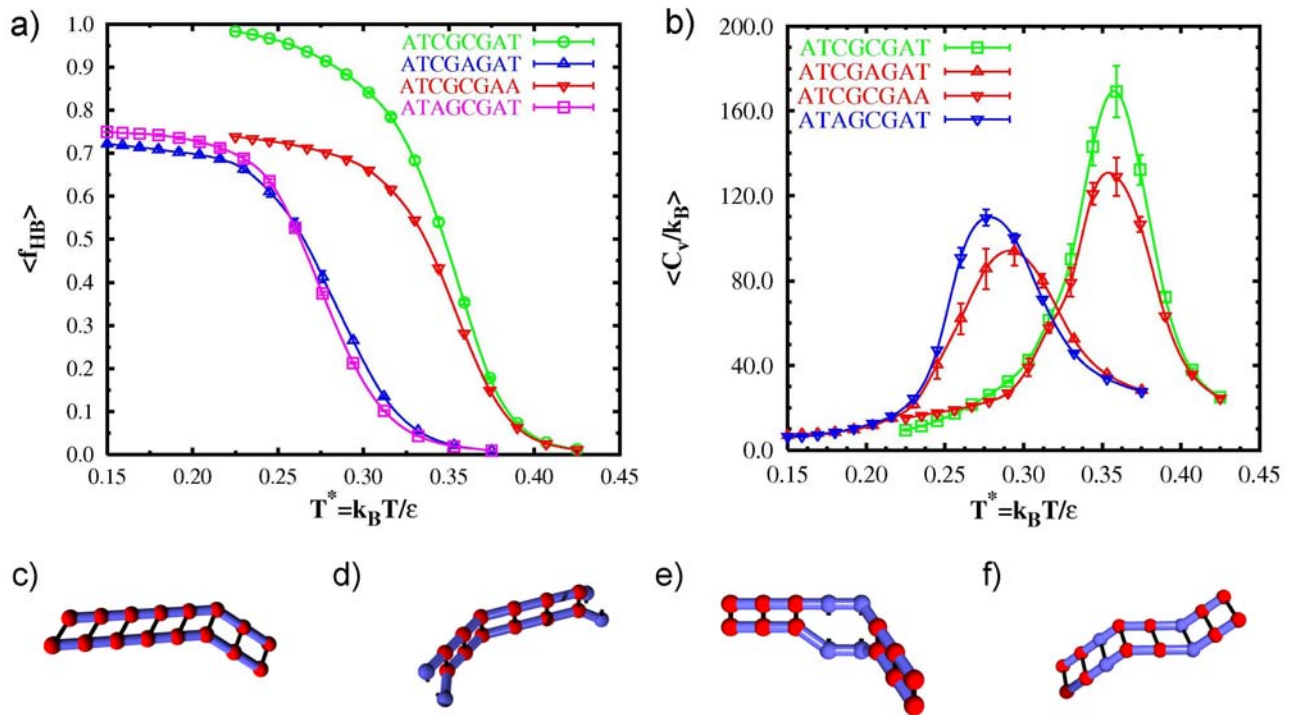


Figure 5. Effect of mismatches on the thermal stability of the self-complementary sequence $(\text{ATCGCGAT})_2$. a) Average fraction of bases bonded $\langle f_{HB} \rangle$ and b) Average specific heat $\langle C_V / k_B \rangle$ as function of the reduced temperature $k_B T / \epsilon$ for: c) non-mismatch (circles), d) end-mismatch (down-triangles), e) center-mismatch (up-triangles) and f) middle-mismatch (squares) sequences. Monomer unit coloring is as described in Fig. 4.

As in the previous case, we performed a sample calculation on the four sequences considered using the DINAMelt server [32] under the same solution conditions. The order and relative value of the melting temperatures obtained from this thermodynamic model are in agreement with the results presented in Fig. 5, i.e., $T_m = 53.9^\circ\text{C}$ (non-mismatch) $\approx T_m =$

53.6°C (end-mismatch) \gg $T_m = 16.6^\circ\text{C}$ (center-mismatch) $>$ $T_m = -0.4^\circ\text{C}$ (middle-mismatch). We also found that even when the center-mismatch sequence is more stable than the middle-mismatch one, the former shows lower cooperativity (wider melting range and lower specific heat peak, see Fig. 5b). Both observations can be explained from the higher degeneracy of the lowest energy configurations coming from the particular arrangement of the sequence with center-mismatch.

The temperature dependence of the fraction of base-pairs in the system can be analyzed with a conventional van't Hoff analysis (two-state model) to obtain the thermodynamic parameters associated to the melting transition [37]. A simple two-state model is commonly assumed in the analysis of melting data from spectroscopic methods (UV absorption or circular dichroism). For sequences much shorter than the persistence length of double-stranded DNA (about 50 base-pairs), this theoretical approximation is fairly reasonable even when the transition is not completely cooperative. In Fig. 6a, we show the effect of strand concentration on the melting transition. The shift observed in the melting temperatures and the increase of the width of the transition (decrease in cooperativity), are in complete agreement with experimental observations [38]. We have performed the same concentration dependence analysis on various self-complementary sequences of different lengths, including cases with dangling ends. As in previous cases, feedback optimized parallel tempering iterations were applied for every sequence at all concentrations studied. The estimation of the precise location of the melting temperatures derives from the multi-histogram reweighting analysis of the specific heat curve.

Excellent linear fits of T_m^{-1} vs. $\log c_T$ are obtained in all the cases studied (as shown in Fig. 6b). These results confirm the validity of the two-state model and provide accurate temperature-independent enthalpy and entropy parameters. The temperature-dependence of the transition $\Delta H_m/k_B$ and $\Delta S_m/k_B$ were also calculated for each sequence (see Figs. 6c and 6d). In general, we observe a good agreement of the thermodynamic parameters calculated from both methods (average enthalpies and entropies are calculated for comparison in the second case). From the slopes of the linear fits in Figs. 6c and 6d, we have also estimated the heat capacity change (ΔC_p) associated with the transition. Following this analysis, we observed that the extent of the specific heat capacity effects, calculated as the ratio $\Delta C_p/\Delta S_m$, is lower than those observed in experiments [38]. Experimentally, this ratio is found to be between 2 and 4, whereas we obtained values in the range of 0 to 1. We argue that this disagreement may originate in the failure of the model parameters, i.e., base-pairing and base-stacking energies, to account correctly for solvation effects related to the double-helix stability in solution. However, it is important to note that thermodynamic parameters determined from spectroscopic methods exhibit discrepancies with respect to calorimetric measurements.

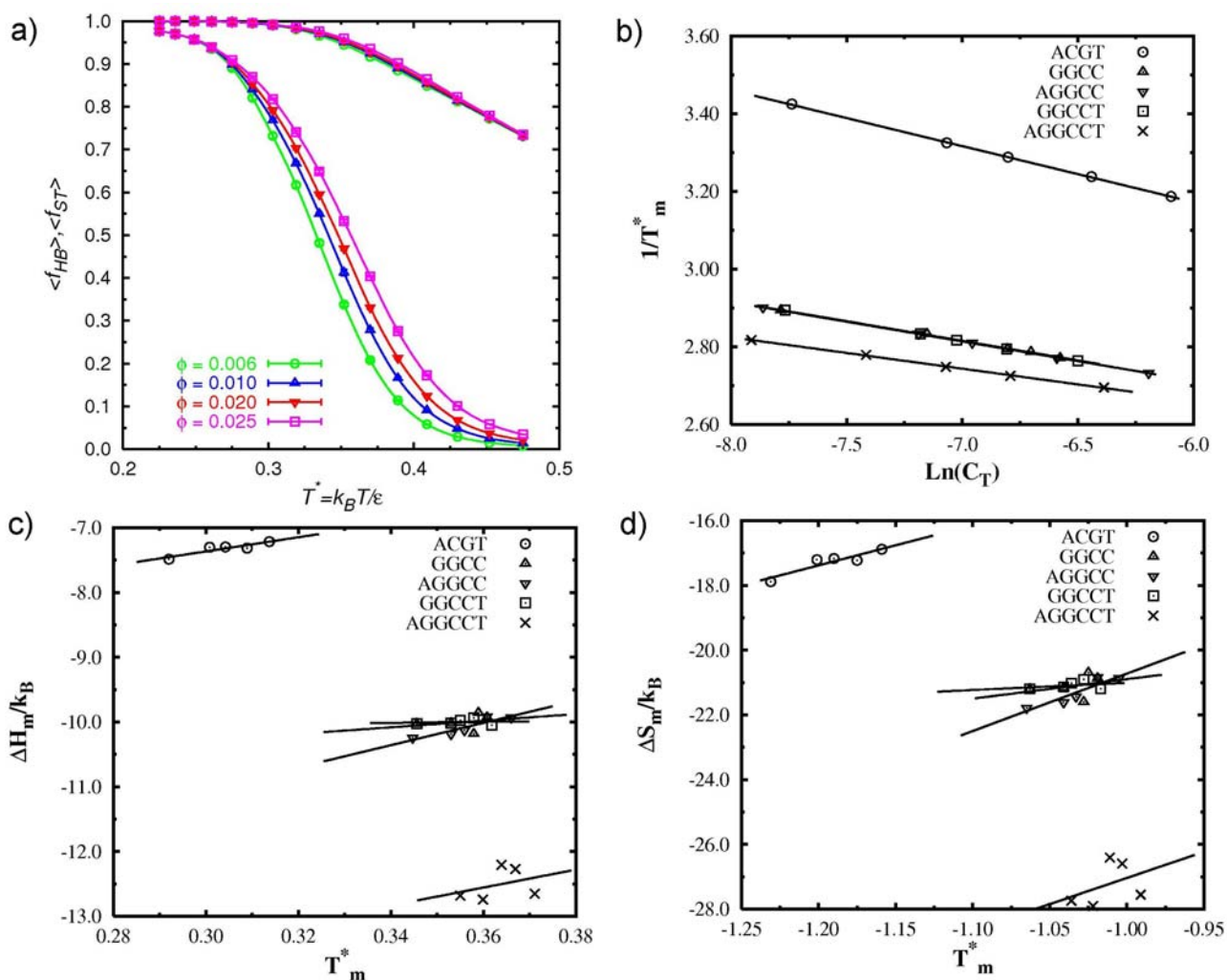


Figure 6. Thermodynamic analysis of the thermal denaturation transition. a) Average fraction of bases bonded $\langle f_{HB} \rangle$ as function of temperature for different concentrations of the self-complementary sequence $(ACGT)_2$; b) Linear fits of T_m^{-1} vs. $\log c_T$ for the sequences $(ACGT)_2$, $(GGCC)_2$, $(AGGCC)_2$, $(GGCCT)_2$ and $(AGGCCT)_2$. c) Linear fits of $\Delta H_m / k_B$ vs T_m for the same sequence on b); d) Linear fits of $\Delta S_m / k_B$ vs T_m for the same sequences on b).

Conclusion

We presented a lattice simulation model to study the thermally-induced denaturation/hybridization transition of DNA chains in solution. The implementation of a multicanonical Monte Carlo approach based on the replica-exchange method, in combination with several biased trials and optimization algorithms, made it possible to bridge the broad time and length scales associated with this transition. The present study clearly indicates that the discretized model developed provides a simple but efficient and rather realistic way to understand the thermodynamic and conformational equilibrium of DNA oligomers in solution. Despite the fact that a quantitative match between experiments and the proposed simulation model is not feasible, a qualitative agreement was found with respect to different experimentally observed phenomena and thermodynamic-based prediction models.

References

1. D.J. Lockhart and E.A. Winzeler. Genomics, gene expression and DNA arrays, *Nature*, 405: 827, 2000.
2. C.M. Niemeyer. Self-assembled nanostructures based on DNA: towards the development of nanobiotechnology, *Curr. Opin. Chem. Biol.*, 4:609, 1999.
3. V.A. Bloomfield, D.M. Crothers, and I. Tinoco. *Nucleic Acids: Structures, Properties and Functions*. University Science Books, Sausalito, California, 2000.
4. J. SantaLucia. A unified view of polymer, dumbbell, and oligonucleotide DNA nearest-neighbor thermodynamics, *Proc. Natl. Acad. Sci.*, 95:1460, 1998.
5. D. Poland and H.A. Scheraga. *Theory of Helix-Coil Transitions in Biopolymers*. Academic Press, New York, 1970.
6. R.G. Larson. Simulations of Self-Assembly, *Curr. Opinion in Coll. Interf. Sci.*, 2:361, 1997.
7. M.D. Frank-Kamenetskii. Biophysics of the DNA molecule, *Phys. Rep.*, 288:13, 1997.
8. K. Binder and W. Paul. Monte Carlo Simulations of Polymer Dynamics: Recent Advances, *J. Poly. Sci. B* 35:1, 1997.
9. P. Jurečka, J. Šponer, J. Černý and P. Hobza. Benchmark database of accurate (MP2 and CCSD(T) complete basis set limit) interaction energies of small model complexes, DNA base pairs, and amino acid pairs, *Phys. Chem. Chem. Phys.*, 8:1985, 2006.
10. J. Šponer, P. Jurečka, I. Marchan, F.J. Luque, M. Orozco and P. Hobza. Nature of Base Stacking: Reference Quantum-Chemical Stacking Energies in Ten Unique B-DNA Base-Pair Steps, *Chem. Eur. J.*, 12:2854, 2006.
11. M. A. Floriano, V. Firetto and A. Z. Panagiotopoulos. Effect of Stiffness on the Phase Behavior of Cubic Lattice Chains, *Macromolecules*, 38:2475, 2005.
12. V. Firetto, M. A. Floriano and A. Z. Panagiotopoulos. Effect of stiffness on the micellization behavior of model H4T4 surfactant chains, *Langmuir*, 22:6514, 2006.
13. N. Korolev, A.P. Lyubartsev, and L. Nordenskiöld. Application of Polyelectrolyte Theories for Analysis of DNA Melting in the Presence of Na⁺ and Mg²⁺ Ions, *Biophys. J.*, 75:3041, 1998.
14. K. Drukker and G.C. Schatz. A Model for simulating dynamics of DNA denaturation, *J. Chem. Phys. B*, 104:6108, 2000.
15. K. Drukker, G. Wu, and G.C. Schatz. Model simulations of DNA denaturation dynamics, *J. Chem. Phys.*, 114:579, 2001.
16. M. Allen and D. Tildesley. *Computer Simulation of Liquids*. Oxford University Press, New York, 1987.
17. R.F. Cracknell, D. Nicholson, N.G. Parsonage and H. Evans. Rotational insertion bias: a novel method for simulating dense phases of structured particles, with particular application to water, *Mol. Phys.*, 71:931, 1990.
18. J.I. Siepmann and D. Frenkel. Configurational bias Monte Carlo: a new sampling scheme for flexible chains, *Mol. Phys.*, 75:59, 1992.

19. D.A. Kofke. Getting the most from molecular simulations, *Mol. Phys.* 102:405, 2004.
20. U.H.E. Hansmann. Parallel tempering algorithm for conformational studies of biological molecules, *Chem. Phys. Lett.*, 281:140, 1997.
21. N. Metropolis, A.W. Rosenbluth, A.H. Rosenbluth, E. Teller, and J. Teller. Equations of state calculations by fast computing machines, *J. Chem. Phys.*, 21:1087, 1953.
22. D.J. Earl and M.W. Deem. Optimal Allocation of Replicas to Processors in Parallel Tempering Simulations, *J. Phys. Chem B*, 108:6844, 2004.
23. D.A. Kofke. On the acceptance probability of replica-exchange Monte Carlo trials, *J. Chem. Phys.* 117:6911, 2002.
24. H.G. Katzgraber, S. Trebst, D.A. Huse and M. Troyer. Feedback-optimized parallel tempering Monte Carlo, *J. Stat. Mech.* P03018, 2006.
25. S. Trebst, M. Troyer and U.H.E. Hansmann. Optimized parallel tempering simulations of proteins, *J. Chem. Phys.*, 124:174903, 2006.
26. A.M. Ferrenberg and R.H. Swendsen. Monte Carlo methods for phase Equilibria of fluids, *Phys. Rev. Lett.*, 61:2635, 1988.
27. A.M. Ferrenberg and R.H. Swendsen. Optimized Monte Carlo data analysis, *Phys. Rev. Lett.*, 63:1195, 1989.
28. J.B. Mills, E. Vacano and P.J. Hagerman. Flexibility of single-stranded DNA: Use of gapped duplex helices to determine the persistence lengths of poly(dT) and poly(dA), *J. Mol. Biol.*, 285:245, 1999.
29. N. Theodorakopoulos. Phase transitions in homogeneous biopolymers: basic concepts and methods, in *Localization and energy transfer in nonlinear systems*, L.Vazquez, R.S. MacKay and M.P. Zorzano (Eds.), pp. 130-152, World Scientific, 2003.
30. T.S. van Erp, S. Cuesta-Lopez, and M. Peyrard. Bubbles and denaturation in DNA, *Eur. Phys. J. E*, 20: 421, 2006.
31. N.A. Alves and U.H.E. Hansmann. Partition function zeros and finite size scaling of helix-coil transitions in a polypeptide, *Phys. Rev. Lett.*, 84:1836, 2000.
32. N.R. Markham and M. Zuker. DINAMelt web server for nucleic acid melting prediction, *Nucleic Acids Res.*, 33:W577-W581, 2005.
33. D. Proschke. Elementary steps of base recognition and helix-coil transitions in nucleic acids, *Mol. Biol. Biochem. Biophys.*, 24:191, 1977.
34. J.H. Gibbs and DiMarzio E.A. Statistical mechanics of helix-coil phase transitions in biological macromolecules, *J. Chem. Phys.*, 30:271, 1959.
35. B.H. Zimm and J.K. Bragg. Theory of phase transitions between helix and random coil in polypeptide chains, *J. Chem. Phys.*, 31:526, 1959.
36. J. Applequist and V. Damle. Theory of the effects of concentration and chain length on helix-coil equilibria in two-stranded nucleic acids, *J. Chem. Phys.*, 39:2719, 1963.

37. R.M. Wartell and A.S. Benight. Thermal denaturation of DNA molecules: a comparison of theory with experiments, *Phys. Rep.*, 126:67, 1985.
38. M. Petersheim, D.H.Turner. Base-stacking and base-pairing contributions to helix stability: thermodynamics of double-helix formation with CCGG, CCGGp, CCGGAp, ACCGGp, CCGGUp, and ACCGGUp, *Biochemistry*, 22:256, 1983.
39. I. Rouzina and V.A. Bloomfield. Heat capacity effects on the melting of DNA: General aspects, *Biophys. J.*, 77:3242, 1999.